Rev. Roum. Sci. Techn.– Électrotechn. et Énerg.
Vol. **67**, *1*, pp. 343–348, Bucarest, 2022

Thermotechnique et thermoénergétique

COOLING SYSTEM FOR PHOTOVOLTAIC PANELS

FLORIN SAFTOIU, ALEXANDRU M. MOREGA

Keywords: Photovoltaic panel; Single flow cooling system; Infrared irradiance; Joule effect; Numerical simulation.

This study focuses on the heating of a PV panel subject to infrared irradiance and the electric load-related Joule effect, as reducing the temperature of the PV panel may increase the PV conversion efficiency. A water-circulated heat exchanger is provided on the back of the PV panel to minimize the hotspot temperature. The heat thus extracted out of the system may be further used in a secondary energy conversion system.

1. INTRODUCTION

One of the significant issues of PV panels is their overheating beyond the functioning limits caused by solar irradiation, the Joule effect, and environmental thermal conditions that lead to diminishing the efficiency of the overall PV conversion and the pending reduction in the electric power available for usage or storage. As a thumb rule, for each unit of extra heat, the electrical efficiency of the PV panel decreases by 0.5 % [1].

Several methods may be used to reduce PV heating, *e.g*., heat pipes, forced flow cooling systems, *etc*. Consistent studies are reported in this domain, ranging from the passive cooling system to the active cooling system, with water as a coolant, *e.g*., [3–5].

The first passive cooling method to mention here is the cooling with a clay pot where the water flows based on the thermal siphon effect through the gap formed on the back of the PV panel [2]. That experiment showed off a promising 10 % increase in efficiency. However, the pressure increases registered in water flow resulted in the bending of PV's front face. This is the reason for marginally lower panel efficiency, 11.6 % for cooled PV panels, compared to the 12.11 % reference PV panel efficiency [2]. Another study of an active (forced) water-cooled PV system [3] includes a water pump and a closed circuit that connects the fluidic circuit provided on the PV panel backside to a water reservoir.

Here we look forward to finding how infrared power and the Joule effect may be harnessed to diminish the PV panel thermal load, on one hand, and the usage of the heat exhausted into a secondary energy conversion system. This study is concerned with a cooling solution that provides for an evenly distributed coolant on the backside of the PV panel, except for the area of the wires' junction box. The efficiency in this case should increase by 25 % [3].

A similar study refers to an interesting cooling method of the PV panel that uses a heat collector with I/O gates on the back of the PV panel, which can be easily operated to obtain the temperature needed on the front face of the cover glass [9]. The configuration (geometry) of the collector, the number of I/O gates, and the cooling fluid flow rate can be adjusted without modifying the hardware solution, only by changing the configuration. Numerical simulations were used to find the optimal design, and the cooling flow rate showed a 1.6 % increase in electrical efficiency [4].

The solution that makes the main difference here is a counterflow heat exchanger with extruded back cover pipes. A related study evaluates the cooling efficiency of a system with extruded back cover single-flow pipes and different coolant types [5]. The whole system (PV panel and the counterflow system) could be seen as a hybrid photovoltaic/thermal (PV/Th) if the reuse of the exhausted thermal power that results from cooling the PV is envisaged.

A similarity analysis evaluation of the cooling performance of a PV, seen as a hot plate cooled by air natural convection, is performed to gain insights into the order of magnitude heat transfer sizing of the PV panel without the counterflow cooling system. The tilt angle of the panel concerning gravity is a crucial control parameter in natural convection, and it may be used to diminish the PV thermal load. The study is extended to forced convection cooling solutions, and numerical simulations (finite element method, FEM) are used in this aim.

2. SIMILARITY ANALYSIS OF THE HEAT TRANSFER FROM THE PV PANEL TO THE AMBIENT

The PV panel is seen here as an inclined hot plate whose tilt angle concerning gravity influences the convection heat transfer to the ambient bathing air. The PV panel is assumed thermally linear, homogeneous, and isotropic. The collector grid may amend these assumptions, but it is thin enough to act as an evenly distributed heat source on the front face of the panel. Depending on the physical circumstances, the PV panel's front face may be assumed either isothermal or constant heat flux ("isoflux"). The front face of the PV panel is assumed "isoflux". However, the numerical simulation results that are obtained may suggest that both conditions are applicable – when active, the collector grid may contribute to this consequence.

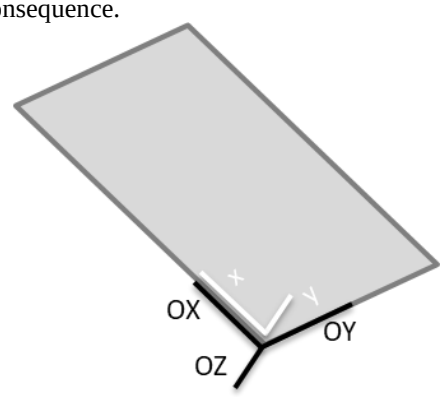

Fig. 1 – The running coordinates, parallel (x) and normal (y) to the plate.

Several empiric studies and mathematical models are devoted to evaluating the thermal performance of this

[1] Doctoral School of Electrical Engineering, "Politehnica" University of Bucharest, Romania, E-mails: florinsaftoiu@gmail.com; amm@iem.pub.ro

convection heat transfer problem, *e.g.*, [6,7]. In the analytic realm, similarity analysis plays an important role. This method provides for first-order accurate, smooth solutions that are confirmed to match closely the experimental results in the order of magnitude sense. The 2D planar coordinates (x,y) – *Oz* is gravity's direction – is replaced by the similarity coordinates (ξ,η) [7]

$$\xi = \left[1 + \frac{\left(\sigma \mathrm{Ra}_L^* \cos\varphi\right)^{1/6}}{\left(\sigma \mathrm{Ra}_L^* |\sin\varphi|\right)^{1/5}}\right]^{-1}, \quad \eta = \lambda \frac{y}{x}, \tag{1}$$

where $\lambda = \left(\sigma \mathrm{Ra}_L^* \cos\varphi\right)^{1/6} + \left(\sigma \mathrm{Ra}_L^* |\sin\varphi|\right)^{1/5}$, $\mathrm{Pr} = \nu/\alpha$ is Prandtl group, $\sigma = \mathrm{Pr}/(1+\mathrm{Pr})$, and

$$\mathrm{Ra}_x^* = \frac{g\beta \cos\varphi \left(q_w \frac{x}{k}\right) x^3}{\alpha\nu} \tag{2}$$

is Rayleigh's number based on *x*. Here g [m/s^2] is the gravitational acceleration; φ [rad] is the tilt angle concerning the horizontal (Fig. 1); β [1/°C] is the volumetric thermal expansion coefficient; q_w [W/m^2] is the wall (front face) heat flux density; x [m] is running coordinate ($x = L$ is the plate length); k [W/mK] is the thermal conductivity of the panel; α [m^2/s] is the thermal diffusivity of the surrounding fluid, and ν [m^2/s] its kinematic viscosity.

The heat transfer group, Nusselt, based on the panel size, *L*, (the characteristic geometric scale), is correlated with the Rayleigh number through [7]

$$\mathrm{Nu}_L = \frac{\left(\mathrm{Ra}_L^* \cos\varphi\right)^{1/6}}{\xi\theta(\xi,0)}. \tag{3}$$

Here $\theta = \lambda(T - T_\infty)/(q_w x/k)$ is the non-dimensional temperature, and T_∞ is the equilibrium temperature of the fluid far away from the plate.

The data compiled in the Annex indicate that $\mathrm{Ra}_L^* = 2.38\times10^7$ for the hot plate (the PV panel here) with uniform flux density front face and insulated back face. For example, Fig. 1 plots $\mathrm{Nu}_L(\mathrm{Ra}_L^*,\varphi)$ for $\varphi = 0$ °. The fluid here is air, for which Pr = 0.7.

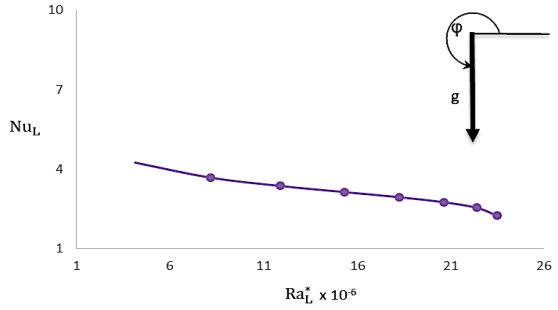

Fig. 2 – Nusselt number vs. Rayleigh number for the horizontal warm plate facing upwards.

The non-dimensional $\mathrm{Nu}_L(\mathrm{Ra}_L^*,\varphi)$ characteristic may provide the convection heat transfer coefficient $h(\varphi)$ [W/(m^{2}K)] that is used next, in numerical simulations (Section 5). Table 1 lists Nu_L and h for $\mathrm{Ra}_L^* = 2.38\times10^7$ for the PV panel cooled by natural convection as functions of the tilt angle, φ, and Fig. 2 renders them graphically.

The heat transfer performance of the PV panel may be sized in the order of magnitude sense using empiric correlation results $\mathrm{Nu}_L(\mathrm{Ra}^*_L,\varphi)$ – Fig. 3.

Table 1

The influence of tilt angle on the heat transfer rate [7]

Tilt angle, φ[°]	$\mathrm{Nu}_L(\mathrm{Ra}_L^*,\varphi)$	h [W/(m^{2}K)]
10	4.25	3.664
20	3.68	3.175
30	3.36	2.903
40	3.13	2.705
50	2.94	2.536
60	2.75	2.373
70	2.54	2.192
80	2.25	1.939

However, numerical simulations may be used to find more accurate results (next section).

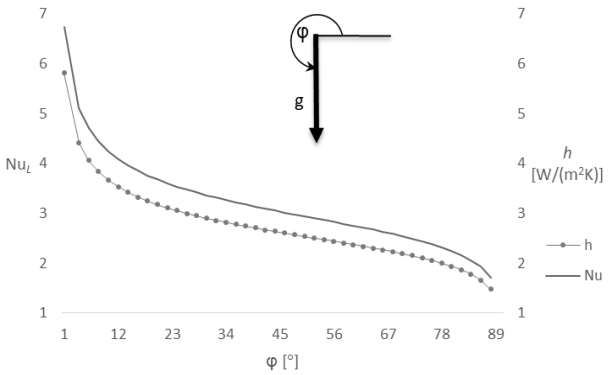

Fig. 3 – Air natural cooling of the PV panel [8] presented through Nu_L (the ordinate at the left) and h (on the right ordinate) for $\mathrm{Ra}^*_L = 2.38\times10^7$.

As expected, the higher the Nu_L group (or h) is the better the cooling effect through natural convection.

This is only one step in the heat management of the PV panel. Next, forced convection is added to the cooling system. This case is analyzed next using numerical simulations. Moreover, radiation heat transfer must be added, and this mechanism is addressed here indirectly by enhancing the convection heat transfer.

3. THE PHOTOVOLTAIC PANEL

The best-case scenario for the PV panel electric power production (the maximum power point, MPP) is simultaneously the worst-case scenario for heat production, which is a menace to its thermal stability. This happens when the external load (resistance), R_e, matches the PV of the internal resistance, R_i [6]. Based on this condition, we advance the analysis of the Joule effect at MPP and the thermal load (temperature distribution) of the PV panel. When present, the cooling pipes will evacuate some amount of heat that will, in turn, reduce the thermal load. At the same time, it increases the overall efficiency of the solar system by providing a supplementary (heat) power source. The PV data used in this study are those of the Solahart panel with 6×20 monocrystalline 'Q.ANTUM solar', which is built using half-cells technology [10]. The parameters that are used in this study are in the Annex.

The cover of the PV panel's front face is made of 3.2 mm thick thermally pre-stressed glass, anti-reflect coating technology, and the back sheet is made of composite film. Its frame is made of black anodized aluminum. The environmental temperature working conditions range from – 40 ºC to + 85 ºC.

4. THE MATHEMATICAL MODEL

A 3D PV panel provided with a counterflow cooling system is analyzed. The heat transfer problem is solved numerically for stationary working conditions using the FEM technique [12]. When present, the flow in the single-current or counter-current systems is assumed stationary and incompressible, and the fluid (water) is Newtonian. In laminar flows, these are [6, 8]

– *momentum conservation*

$$\rho(\mathbf{u}\cdot\nabla)\mathbf{u} = \nabla\cdot\left[-p\mathbf{I} + \eta\left(\nabla\mathbf{u} + (\nabla\mathbf{u})^{\mathrm{T}}\right)\right], \tag{4}$$

– *mass conservation*

$$\nabla\cdot\mathbf{u} = 0, \tag{5}$$

where **u** [m/s] is the velocity field, p [Pa] is the pressure, and η [Pa·s] is the dynamic viscosity.

For turbulent flow conditions, we use the κ-ω model, which is recommended when

– *momentum balance*

$$\rho(\mathbf{u}\cdot\nabla)\mathbf{u} = \nabla\cdot\begin{bmatrix} -p\mathbf{I} + (\eta+\eta_{\mathrm{T}})(\nabla\mathbf{u} + (\nabla\mathbf{u})^{\mathrm{T}}) \\ -\nabla\cdot\left[\frac{2}{3}(\eta+\eta_{\mathrm{T}})(\nabla\cdot\mathbf{u})\mathbf{I}\right] \end{bmatrix},$$

where the last term in eq. (1), $\nabla\cdot\left[\frac{2}{3}(\eta+\eta_T)(\nabla\cdot\mathbf{u})\mathbf{I}\right]$, is enabled only for Ma < 0.3.

– *RANS equation for the turbulence kinetic energy balance*

$$(\rho\mathbf{u}\cdot\nabla)\kappa = P - \beta^{*}\rho\kappa\omega + \nabla\cdot[(\eta + \sigma_{\mathrm{k}}\rho\kappa/\omega)\nabla\kappa],$$

– *RANS equation for the specific rate of dissipation of kinetic energy balance*

$$(\rho\mathbf{u}\cdot\nabla)\omega = \frac{\alpha\omega}{\mathrm{k}}P - \beta\rho\omega^2 + \nabla\cdot[(\eta + \sigma_{\omega}\rho\kappa/\omega)\nabla\omega],$$

– *mass balance*

$(\nabla\cdot\rho\mathbf{u})=0$, for compressible flow,

$\rho\nabla\cdot\mathbf{u} = 0$, for incompressible flow.

Here **u** [m/s^2] is the velocity, p [N/m^2] the pressure, ρ [kg/m^3] the mass density, ν [s^{-1}] the dynamic viscosity, **I** the unity matrix, $\mathrm{P}(\mathbf{u})=(\rho\kappa/\omega)\left[\nabla\mathbf{u}:(\nabla\mathbf{u}+(\nabla\mathbf{u})^{\mathrm{T}}) - \frac{2}{3}(\nabla\cdot\mathbf{u})^2\right] - \frac{2}{3}\rho\kappa\nabla\cdot\mathbf{u}$, Ma = $|\boldsymbol{u}|/a_{\mathrm{air}}$ is the local Mach number, a_{air} [m/s] is the velocity of the sound in the air, and κ [J/kg] is the turbulent kinetic energy. The eddy viscosity required by the RANS equations is $\nu_T = \kappa/\omega$. The recommended values for the different parameters are available, *e.g.*, in [11].

The boundary conditions that close the model is the following: the input velocity of the cooling fluid is set from 1 to 8 m/s; the output pressure is 0 bar, and the pipe walls are "no-slip" (zero velocity).

A typical quantity in the fluid mechanics of forced flows is the Reynolds group [6]

$$\mathrm{Re}_D = \frac{\rho UD}{\eta}, \tag{6}$$

where D [m] is the characteristic length scale, and U [m/s] is the velocity scale. This group may be used to evaluate, *a priori*, the type of flow, laminar or turbulent. For duct flows, D is the (hydraulic) diameter, and U is the cross-sectional averaged velocity. Here Re_D = (1800 to 14400), which indicates that the flow is laminar (for the lower velocities) and substantiates the validity of the model (4), (5) (see Table 6 of the Annex).

The heat transfer part of the model is governed by the energy equation [8]

$$\rho c_p(\mathbf{u}\cdot\nabla)T = \nabla(k\nabla T) + Q, \tag{7}$$

where c_P [J/kg·K] is the specific heat at constant pressure, and [W/m^3] is the heat source inside the PV panel, by the Joule effect, which adds the equivalent of the absorbed portion of the solar IR radiation intake.

The environmental thermal constraints are convection heat transfer (constant h) on the PV front and backsides and thermal insulation for the lateral frame of the PV panel. The total front face irradiation, including the IR portion, is assumed to be 1000 W/m^2, the inlet temperature of the cooling agent (water) is 20 °C, and its exit is considered homogeneous conduction (heat is transferred by convection only).

To have a meaningful example of how a cooling system works, two design solutions are chosen: the PV panel with and without cooling systems. In both cases, the heating is due to the infrared irradiation and the Joule effect in the maximum power point (MPP) circumstances.

5. NUMERICAL SIMULATION RESULTS

This chapter is dedicated to the numerical simulations of the PV panel cooled by natural convection with and without a supplementary cooling system.

5.1. NATURAL CONVECTION COOLING

This solution has no pipes active. It can be seen in Fig. 4 that the PV panel is naturally cooled without any cooling system. Comparing this model with the analytical study, we can observe that the similarity analysis from Lin's study [7], especially h ratio is almost the same.

Tables 2 and 3 help us to read the graphs in the way of conversion between tilt angle, φ vs convection heat transfer coefficient, h and power coefficient, P vs. thermal power of the PV panel, P_n.

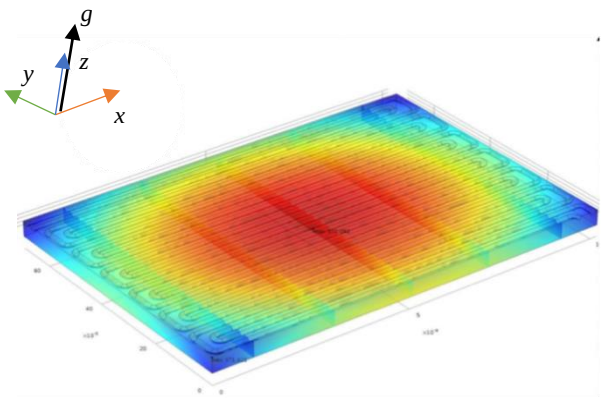

Fig. 4 – Temperature distribution on the surface of back side of the PV panel for natural convection solution without cooling pipe system – T_{max} = 98.95 °C, T_{min} = 98.65 °C. The panel is upside down.

On the other hand, for this design (the PV without supplementary counterflow cooling), the highest temperature is 98.95 ºC, and the lowest temperature is 98.65 ºC, *i.e.*, the panel is almost isothermal. This result confirms, *a posteriori*, that the similarity analysis results, *e.g.*, [7], and the experimental correlations method, *e.g.*, [6], are both acceptable because the PV panel is, at the same time, both (almost) isothermal and with uniform heat flux.

Table 2

The PV panel tilt angle *vs.* the heat transfer coefficient

φ [°]	10	20	30	50	70	80
h [W/m^{2}K]	3.66	3.18	2.9	2.54	2.19	1.94

Table 3

The power factor coefficient P *vs.* the thermal power density on the panel surface P_n

P [-]	0.5	0.7	0.9	1
P_n [W/m^2]	3966	5552	7138	7932

Figure 4 shows the hot spot temperature, on the front face of the PV panel, for this model – without the counterflow cooling system, for natural convection and natural convection cooling plus IR dissipation.

When the IR heat transfer is accounted for a slight difference between those two curves from the above graphic. As the PV panel angle increase, the IR participation in heat dissipation increase as well.

5.2. FORCED CONVECTION COOLING

The PV panel cooled by force convection systems shows off the highest outlet temperature 81.37 ºC for a single-current flow cooling system (U_{in} = 0.02 m/s). The lowest temperature is about 20 ºC – the inlet temperature of the cooling water. The results for the counterflow cooling system will be presented in a future paper.

In this situation, the PV panel is served with a single pipe, Fig. 5 (the panel is presented upside down).

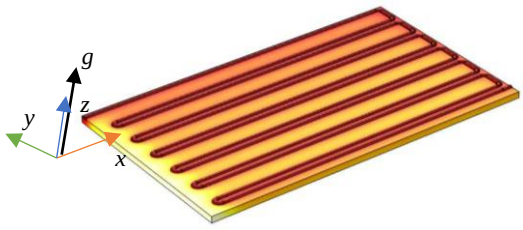

Fig. 5 – Temperature distribution on the surface of back side of the PV panel for single flow solution – P_n = 7932 W/m^2, U_{in} = 1 m/s.

Figure 6 shows the thermal power of the panel P_n = = 7932 W/m^2 is constant, but the inlet velocity of the cooling fluid is variable between 0.02 – 2 m/s. The PV panel is isothermal, which means the water-cooling system extracts a constant amount of heat all over its path.

Table 4

The thermal power extracted by the cooling system, $\dot{Q}$, and mechanical work, $\dot{W}$, for single laminar (ns) and turbulent (κ-ω) flows

U_{in} [m/s]	T [°C]	ΔT [°C]	$\dot{Q}$ [W]	Flow rate [kg/s]	$\dot{W}$ [W]	Re$_D$
0.02	81.37	61.37	5.62	0.004	1.32	351
0.05	56.97	36.97	13.03	0.009	3.31	878
0.1	46	26	25.14	0.019	6.61	1757
0.11	44.78	24.78	28.5	0.021	7.53	2000
0.17	43.78	23.78	42.61	0.032	11.29	3000
0.2	26.29	6.29	46.97	0.037	13.23	3514
0.5	24.5	4.5	116.67	0.093	33.07	8784
1	23.7	3.7	232.68	0.186	66.14	17569
2	22.73	2.73	463.72	0.373	132.27	35138

As expected, the mechanical work is proportional to the inlet velocity.

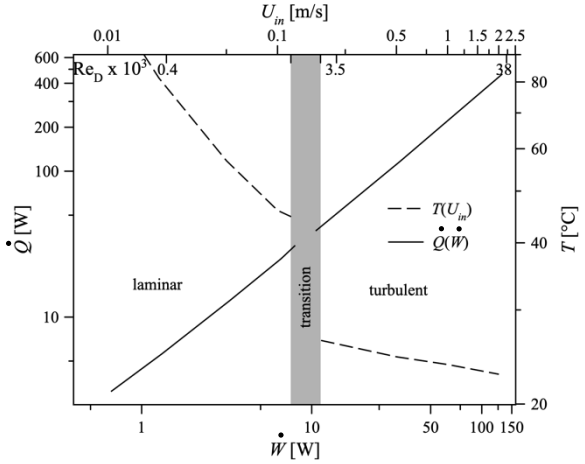

Fig. 6 – The mechanical power needed for different input velocities U_{in}, when h = 1.94 W/(m^{2}K).

On the other hand, thermal power, $\dot{Q}$, that can be extracted from the water, reaches the limit when economical studies occur. Figure 7 shows the efficiency of the thermal power extraction over the mechanical work required to pump the cooling agent.

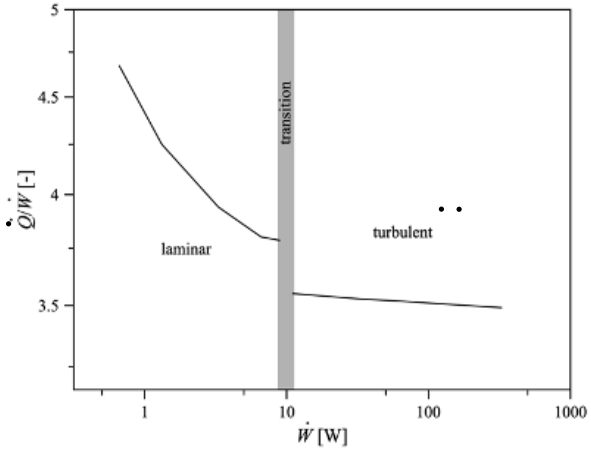

Fig. 7 – The mechanical power needed for different input velocities U_{in}, when h = 1.94 W/(m^{2}K).

Figures 8 and 9 show the PV panel temperature in particular directions, which confirms that the panel (Fig. 5) is almost isothermal, except for the region of the cooling system inlet. There are different curves for different input velocities that could satisfy the isothermal condition.

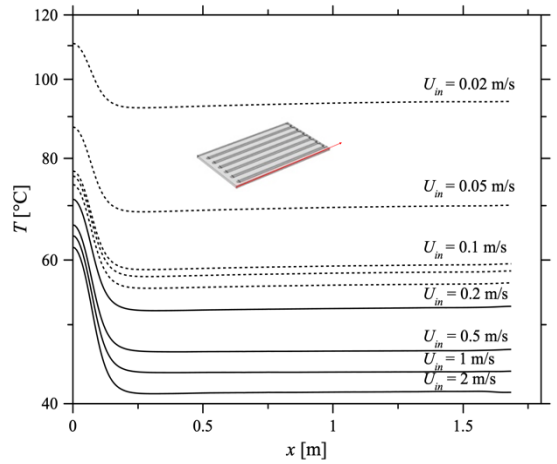

Fig. 8 – T along $y|_{x=0}$ for different inlet velocities.

Besides, it can be observed the influence of cooling pipes that introduces a fluctuation in the PV panel temperature over the areas that are closer to the pipe.

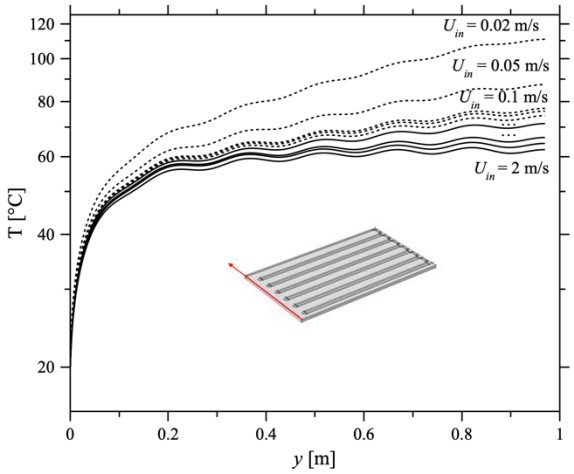

Fig. 9 – T along $y|_{x=0}$ (Fig. 1) for different input velocities.

Both curves in Fig. 10 show that the PV panel temperature decreases with h increase. The inlet velocity is constant (U_{in} = 1 m/s) for each convection heat transfer coefficient, h (related to Fig. 5). This confirms that the h is directly responsible for the PV panel cooling.

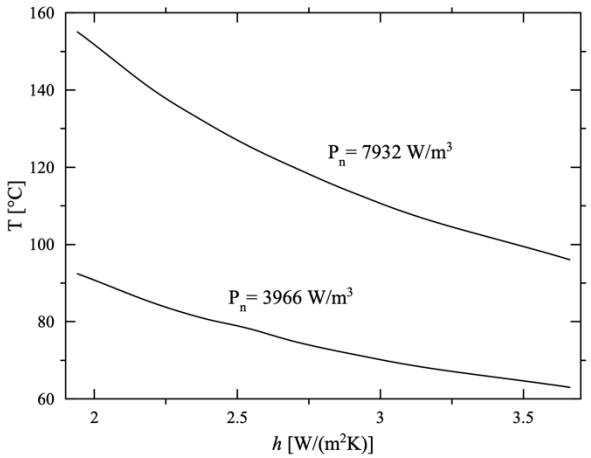

Fig. 10 – T versus h for single flow cooling method.

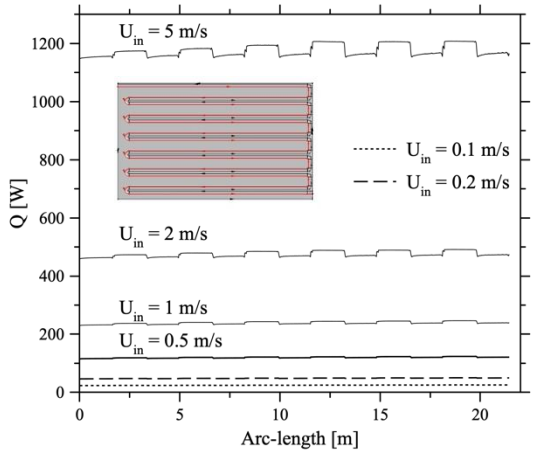

Fig. 11 – Thermal energy - $\dot{Q}$ [W], extracted from the PV panel by the cooling pipe's trace in a single flow for different input coefficients – U_{in}.

Figure 11 shows the PV panel extracted thermal heat based on the different inlet velocities for h = 1.94 W/m^{2}K (related to Fig. 5). It can be seen the fact that the PV panel temperature increase on the pipe elbow area. The cooling system collects thermal heat from the PV panel until it reaches an almost isothermal state. As the fluid has more velocity it can extract from the pipe wall that interacts with the back of the PV panel the heat from its volume.

6. CONCLUSIONS

Joule effect and infrared energy is heating the PV panel to 98.95 ºC. Natural convection is seemingly not an option to extract thermal power for further usage.

On adding the cooling pipes on the back of the PV panel, the outlet temperature from the cooling system is about 92 ºC (for one way solution, P_n = 7932 W/m^2, U_{in} = 1 m/s). That means the cooling pipes evacuate an amount of heat that reduces the temperature of the PV panel.

The turbulent flow cooling provides for better cooling (Fig. 7). However, the thermal power extracted by the cooling system decreases with the flow rate. Seemingly, there is an optimum, a trade-off, between cooling (lower temperature) vs. thermal power, which makes it the object of future research.

The work on a counterflow cooling system is in progress, and the results will be reported soon.

Moreover, by using a PLC device that facilitates the remote control and data collection, it can operate the valve of each pipe and adjust the inlet velocity to obtain the best performance. Together with a remote electrical tilt servo engine, this solution will be implemented with all its features in the following projects to validate this study.

ANNEX

Table 7

Parameters and properties – compiled from [11]

Empiric Parameter	Value
q_w – irradiance, power density	1000 W/m^2
c_p – specific heat of the PV panel	4.181 kJ/kg·K
η – dynamic viscosity of water	0.797 mPa·s
ρ – fluid density	0.994 g/cm^3
η_0 – optical efficiency	0.803
α – thermal diffusivity of the fluid	2.21x10^{-5} m^2/s
ν – kinematic viscosity of fluid	1.61x10^{-5} m^2/s

Table 8

Parameters of the cooling system

Parameter	Value
T_{in} – fluid input temperature	20 °C
D – diameter of the pipe	15.4 mm
A_p – cross sectional area of the pipe	47.17 mm^2
U_{in} – inlet velocity in the counter-flow system	0.02–2 m/s
Re_D –Reynolds number	351-35138

Table 9

PV panel data sheet [10]

Parameter	Value
P_{MPP} – maximum power point (MPP)	285 W
I_{sc} – short-circuit current	9.46 A
V_{oc} – open circuit voltage	39.22 V
I_{MPP} – current at the MPP	8.91 A
V_{MPP} – voltage at the MPP	31.99 V
η – electrical efficiency	17.1 %
R_i – internal electrical resistance of the PV panel	3.18 Ω

ACKNOWLEDGMENTS

The numerical simulations were conducted in the Laboratory for Multiphysics Modeling at the Faculty of Electrical Engineering, UPB.

Received on 9 September 2022

REFERENCES

1. K.A. Moharram, M.S. Abd-Elhady, H.A. Kandil, H. El-Sherif, *Enhancing the performance of photovoltaic panels by water cooling*, Ain Shams Engineering Journal, **4**, *4*, pp. 869–877, 2013.
2. W. Owhaib, Y. Qanadah, H. Al-Ajalin, A. Tuffaha, W. Al-Kouz, *Photovoltaic panel efficiency improvement by using direct water passive cooling with clay pot*, International Renewable Engineering Conference (IREC), **12**, pp. 1–4 (2021).
3. S.A. Saada, I. Kecili, R. Nebbali, *Preliminary study of a water-cooled PV system*, International Conference on Communications and Electrical Engineering (ICCEE), 2018, pp. 1–4.
4. C. Hajjaj, H. Amiry, R. Bendaoud, S. Yadir, A. Elhassnaoui, S. Sahnoun, M. Benhmida, A. El Rhassouli, *Design of a new photovoltaic panel cooling system to optimize its electrical efficiency*, International Renewable and Sustainable Energy Conference (IRSEC), 2016, pp. 623–627.
5. D. Adhya, S. Bhattacharjee, S. Acharya, *Back surface cooling of photovoltaic panel – an experimental investigation*, IEEE International Conference on Power Systems (ICPS), **6**, *1*, 2016, pp. 1–6.
6. A. Bejan, *Heat Transfer*, John Wiley & Sons, Inc., New York, 1993.
7. H.T. Lin, W.S. Yu, S.L Yang, *Free convection on an arbitrarily inclined plate with uniform surface heat flux*, Wärme und Stofffübertragung, **24**, 1989, pp.183–190.
8. A.M. Morega, *Principles of Heat Transfer*, Chapter VII in *Mechanical Engineer's Handbook*, Ed. D.B. Marghitu, Academic Press, 2001, pp. 446–455,.
9. A.M. Morega, *Energy Sources*, Lecture Notes, UPB, 2020.
10. *Solahart Data Sheet*, ih0113_qcells_qplus-g43_285w_april-2019_web (2019).
11. A.M. Morega, *Photovoltaic Systems*, Lecture Notes, UPB, 2020.
12. Comsol Multiphysics v. 5.6a, *Release Notes*, 2021.